

TITLE PAGE

1
2
3
4
5
6
7
8
9
10
11
12
13
14
15
16
17
18
19
20
21
22
23
24
25

Type of article: Research article

Full-length title:

Culture and identification of a “Deltamicon” SARS-CoV-2 in a three cases cluster in southern France

Short title (for the running head): Emergence of a SARS-CoV-2 Delta/Omicron recombinant

Author list: Philippe COLSON^{1,2,3} *, Pierre-Edouard FOURNIER^{1,2,4}, Jeremy DELERCE¹, Matthieu MILLION^{1,2,3}, Marielle BEDOTTO¹, Linda HOUHAMDI¹, Nouara YAHY⁵, Jeremy BAYETTE⁶, Anthony LEVASSEUR^{1,2}, Jacques FANTINI⁵, Didier RAOULT^{1,2}, Bernard LA SCOLA^{1,2,3} *

Affiliations: ¹ IHU Méditerranée Infection, 19-21 boulevard Jean Moulin, 13005 Marseille, France; ² Aix-Marseille Univ., Institut de Recherche pour le Développement (IRD), Microbes Evolution Phylogeny and Infections (MEPHI), 27 boulevard Jean Moulin, 13005 Marseille, France; ³ Assistance Publique-Hôpitaux de Marseille (AP-HM), 264 rue Saint-Pierre, 13005 Marseille, France; ⁴ Aix-Marseille Univ., Institut de Recherche pour le Développement (IRD), Vecteurs – Infections Tropicales et Méditerranéennes (VITROME), 27 boulevard Jean Moulin, 13005 Marseille, France; ⁵ Aix-Marseille Université, INSERM UMR S 1072, 51 boulevard Pierre Dramard, 13015 Marseille, France; ⁶ LBM Inovie Labosud, 90 rue Nicolas Chedville, 34070, Montpellier, France.

*** Corresponding author:** Bernard La Scola, IHU Méditerranée Infection, 19-21 boulevard
NOTE: This preprint reports new research that has not been certified by peer review and should not be used to guide clinical practice.

26 Jean Moulin, 13005 Marseille, France. Tel.: +33 413 732 401, Fax: +33 413 732 402; email:

27 bernard.la-scola@univ-amu.fr; Philippe Colson, IHU Méditerranée Infection, 19-21

28 boulevard Jean Moulin, 13005 Marseille, France. Tel.: +33 413 732 401, Fax: +33 413 732

29 402; email: philippe.colson@univ-amu.fr

30 **Key words:** SARS-CoV-2; recombinant; variant; lineage; Delta; Omicron; Deltamicron;

31 epidemic

32 **Word counts:** abstract, 180; text, 2,364

33 **Figures:** 3; **Table:** 1; **References:** 47

34

35

36
37
38
39
40
41
42
43
44
45
46
47
48
49
50
51
52
53
54

ABSTRACT

Multiple SARS-CoV-2 variants have successively, or concomitantly spread worldwide since summer 2020. A few co-infections with different variants were reported and genetic recombinations, common among coronaviruses, were reported or suspected based on co-detection of signature mutations of different variants in a given genome. Here we report three infections in southern France with a Delta 21J/AY.4-Omicron 21K/BA.1 “Deltamicron” recombinant. The hybrid genome harbors signature mutations of the two lineages, supported by a mean sequencing depth of 1,163-1,421 reads and mean nucleotide diversity of 0.1-0.6%. It is composed of the near full-length spike gene (from codons 156-179) of an Omicron 21K/BA.1 variant in a Delta 21J/AY.4 lineage backbone. Importantly, we cultured an isolate of this recombinant and sequenced its genome. It was observed by scanning electron microscopy. As it is misidentified with current variant screening qPCR, we designed and implemented for routine diagnosis a specific duplex qPCR. Finally, structural analysis of the recombinant spike suggested its hybrid content could optimize viral binding to the host cell membrane. These findings prompt further studies of the virological, epidemiological, and clinical features of this recombinant.

55

TEXT

56

57 **Introduction**

58 The current SARS-CoV-2 pandemic has highlighted since the summer of 2020 the
59 successive or concomittant emergence of numerous viral variants, each causing a specific
60 epidemic.¹⁻³ Some of these variants spread to become pandemic while others remained
61 epidemic in a restricted geographical area. The variants characterized so far have been shaped
62 by nucleotide substitutions, insertions or deletions. However, another major evolutionary
63 mechanism of RNA viruses is genetic recombination, which is very common among
64 coronaviruses.⁴⁻⁸ It requires co-infection of the same host cell by two viruses, which may be
65 two distinct mutants or variants.⁹ Therefore, the frequency of creation of recombinants
66 between two variants depends on the duration of their co-circulation, on the time until viral
67 clearance, and on the number of people exposed to both viruses. Co-infections with two
68 variants were reported including recently with SARS-CoV-2 Delta and Omicron variants.¹⁰⁻¹³
69 Furthermore, genetic recombinations were reported or suspected, based on the concurrent
70 detection in consensus genomes of signature mutations of different mutants or variants.^{10,12,14-}
71 ²⁴ A study detected up to 1,175 (0.2%) putative recombinant genomes among 537,360
72 genomes and estimated that up to 5% SARS-CoV-2 having circulated in the USA and UK
73 could be recombinants.¹⁶

74 Two pandemic variants, Delta and Omicron 21K (Nextclade classification^{25,26})/BA.1
75 (Pangolin classification²⁷), recently succeeded each other as the predominant viruses but co-
76 circulated for a period of several weeks, creating conditions for co-infections and
77 subsequently recombinations. This period spanned between December 27th, 2021 and
78 February 14th, 2022 in our geographical area, as assessed by our SARS-CoV-2 genotypic
79 surveillance based on variant-specific qPCR and next-generation genomic sequencing.^{3,28,29} In

80 January 2022, genomes harboring mutations from both Delta and Omicron 21K/BA.1 variants
81 were reported in Cyprus but it was questioned whether sequences might have resulted from
82 contamination.²³ Still, 15 genomes as of 27/02/2022 being hybrids of these two variants and
83 highly similar between each other were reported since February 2022 ([https://github.com/cov-
84 lineages/pango-designation/issues/444](https://github.com/cov-lineages/pango-designation/issues/444)). We herein report three infections by a recombinant
85 SARS-CoV-2 Delta 21K/AY.4-Omicron 21K/BA.1 whose genome is highly similar to the 15
86 previously reported genomes and the isolation of the recombinant virus from one of the
87 patients.

88

89 **Materials and methods**

90 Nasopharyngeal samples were collected from two patients in our university hospital
91 institute (Méditerranée Infection; <https://www.mediterranee-infection.com/>) and tested for
92 SARS-CoV-2 infection by real-time reverse transcription-PCR (qPCR) as previously
93 described.^{3,28,29} The third patient was sampled in a private medical biology laboratory in
94 southern France (Inovie Labosud, Montpellier, France). qPCR assays that screen for SARS-
95 CoV-2 variants were performed as recommended by French public health authorities
96 ([https://www.data.gouv.fr/fr/datasets/donnees-de-laboratoires-pour-le-depistage-indicateurs-
97 sur-les-mutations/](https://www.data.gouv.fr/fr/datasets/donnees-de-laboratoires-pour-le-depistage-indicateurs-sur-les-mutations/)). In our center this included the detection of spike mutation among which
98 K417N (Thermo Fisher Scientific, Waltham, USA), combined with testing with the TaqPath
99 COVID-19 kit (Thermo Fisher Scientific) that target viral genes ORF1, N (nucleocapsid) and
100 S (spike), as previously reported.^{3,28,29} The private medical laboratory used the ID SARS-
101 CoV-2/VOC Revolution Pentaplex assay (ID Solutions, Grabels, France) that detects spike
102 mutations K417N, L452R, and E484K (Pentaplex assay, ID Solution, France).

103 SARS-CoV-2 genomes were sequenced in the framework of genomic surveillance
104 implemented since February 2020³ in our institute. Next-generation sequencing was

105 performed with the Illumina COVID-seq protocol on the NovaSeq 6000 instrument (Illumina
106 Inc., San Diego, CA, USA) or with the Oxford Nanopore technology (ONT) on a GridION
107 instrument (Oxford Nanopore Technologies Ltd., Oxford, UK) combined with prior multiplex
108 PCR amplification according to the ARTIC procedure (<https://artic.network/>), as previously
109 described,^{3,28} with the ARTIC nCoV-2019 Amplicon Panel v4.1 of primers (IDT, Coralville,
110 IA, USA). Then, sequence read processing and genome analysis were performed as
111 previously described.^{3,28} Briefly, for Illumina NovaSeq reads, base calling was performed
112 with the Dragen Bcl Convert pipeline [v3.9.3;
113 https://emea.support.illumina.com/sequencing/sequencing_software/bcl-convert.html
114 (Illumina Inc.)], mapping was performed with the bwa-mem2 tool (v. 2.2.1;
115 <https://github.com/bwa-mem2/bwa-mem2>) on the Wuhan-Hu-1 isolate genome (GenBank
116 accession no. NC_045512.2) then cleaned with Samtools (v. 1.13; <https://www.htslib.org/>),
117 variant calling was carried out with freebayes (v. 1.3.5;
118 <https://github.com/freebayes/freebayes>) and consensus genomes were built using Bcftools (v.
119 1.13; <https://samtools.github.io/bcftools/bcftools.html>). ONT reads were processed with the
120 ARTIC-nCoV-bioinformaticsSOP pipeline v1.1.0 ([https://github.com/artic-
121 network/fieldbioinformatics](https://github.com/artic-)). Nucleotide and amino acid changes relatively to the Wuhan-
122 Hu-1 isolate genome were obtained using the Nextclade tool
123 (<https://clades.nextstrain.org/>).^{25,26} Nextstrain clades and Pangolin lineages were determined
124 using the Nextclade web application (<https://clades.nextstrain.org/>)^{25,26} and the Pangolin tool
125 (<https://cov-lineages.org/pangolin.html>),²⁷ respectively. Genome sequences described here
126 were deposited in the GenBank sequence database (<https://www.ncbi.nlm.nih.gov/genbank/>)³⁰
127 (OM990851, OM990852, OM991095, OM991295), and on the IHU Méditerranée Infection
128 website (<https://www.mediterranee-infection.com/sars-cov-2-recombinant/>). The Simplot
129 software (<https://sray.med.som.jhmi.edu/SCROftware/SimPlot/>)³¹ was used for recombination

130 analysis. Phylogeny was reconstructed by the IQTree (v2.1.3; <http://www.iqtree.org/>)³² or
131 MEGA X³³ (v10.2.5; <https://www.megasoftware.net/>) tools and visualized with MEGA X
132 after sequence alignment with MAFFT (<https://mafft.cbrc.jp/alignment/server/>).³⁴ As
133 phylogenetic analysis can hardly applies to sequences that have different evolutionary
134 histories, we built two separate trees, a first one for the regions classified as of the Delta
135 21J/AY.4 variant (positions 1-22,128 and 25,519-29,903 in reference to the genome of the
136 Wuhan-Hu-1 isolate), and a second one for the regions classified as of the Omicron 21K/BA.1
137 variant (positions 22,129-25,519). The 10 genomes the closest genetically to these fragments
138 of the genome obtained here were selected through a BLAST³⁵ search among genomes of the
139 Delta 21J/AY.4 and Omicron 21K/BA.1 variants in the sequence database of our institute that
140 contains approximately 50,000 SARS-CoV-2 genomes; then, they were incorporated in the
141 phylogeny together with the genome of the Wuhan-Hu-1 isolate. As a matter of fact, it should
142 not be acceptable to make a phylogenetic tree based on concatenation of sequences from
143 different origin.

144 SARS-CoV-2 culture isolation was performed by inoculating 200 μ L of respiratory
145 sample on Vero E6 cells as previously described.³⁶ Cytopathic effect was observed by
146 inverted microscopy. Viral particles were visualized in the culture supernatant by scanning
147 electron microscopy with a SU5000 microscope (Hitachi High-Technologies Corporation,
148 Tokyo, Japan), as previously described.³⁷

149 Structural predictions of the spike protein were performed as previously
150 described.^{28,38,39} Briefly, amino acid changes were introduced in the framework of a complete
151 14-1,200 structure of the original SARS-CoV-2 20B spike and missing amino acids were
152 incorporated with the Robetta protein structure prediction tool (<https://rosetta.bakerlab.org/>)
153 before energy minimization through the Polak-Ribière algorithm.

154 A in house duplex qPCR assay specific of the SARS-CoV-2 recombinant was

155 designed that targets the genomes of the Delta 21J [targeted mutation: A11201G in the Nsp6
156 gene (corresponding to amino acid substitution T77A)] and the Omicron 21K/BA.1 [targeted
157 mutations: A23040G, G23048A, A23055G in the spike gene (Q493R, G496S, Q498R)]
158 variants. The sequences of the primers and probes (in 5'-3' orientation) are as follows: (i) for
159 the Delta 21J-targeting system: forward primer, CTGCTTTTGCAATGATGTTTGT; reverse
160 primer, TACGCATCACCCAAGTAGCA; probe, 6FAM-
161 CTTGCCGCTGTAGCTTATTTTAAT (primers and probe concentrations in the mix were
162 200 nM and 150 nM, respectively); (ii) for the Omicron 21K/BA.1-targeting system: forward
163 primer, CCTTGTAATGGTGTGAAGGTTTT; reverse primer,
164 CTGGTGCATGTAGAAGTTCAAAG; probe, 6VIC-
165 TTTACGATCATATAGTTTCCGACCC (primers and probe concentrations in the mix were
166 250 nM and 200 nM, respectively).

167 This study was approved by the ethics committee of University Hospital Institute
168 Méditerranée Infection (No. 2022-001).

169

170 **Results**

171 The three case-patients were SARS-CoV-2-diagnosed on nasopharyngeal samples
172 collected in February 2022. Cycle threshold values (Ct) of diagnostic qPCR were between 20-
173 21. The patients were below 40 years of age. They resided in southern France and did not
174 travel abroad recently. They presented mild respiratory symptoms. Two were vaccinated
175 against SARS-CoV-2 (with two or three doses administered). Variant screening qPCR for the
176 2 samples collected in our institute showed positivity for the K417N mutation while the
177 TaqPath COVID-19 kit provided positive signals for all three genes targeted (ORF1, S, and
178 N). The third sample showed positivity for the K417N mutation and negativity for the L452R
179 and E484K mutations. Thus, overall, qPCR carried out on the three samples were indicative

180 of a Omicron variant.

181 The three viral genomes [GenBank Accession no. OM990851, OM990852,
182 OM991095 (<https://www.ncbi.nlm.nih.gov/genbank/>)³⁰; available on the IHU Méditerranée
183 Infection website (<https://www.mediterranee-infection.com/sars-cov-2-recombinant/>)] were
184 hybrids of Delta 21J/AY.4 and Omicron 21K/BA.1 variant genomes (**Figures 1a, b, c; Table**
185 **1**). At positions harboring mutations compared to the genome of the Wuhan-Hu-1 isolate,
186 mean sequencing depth was between 1,163-1,421 reads and mean prevalence of the
187 majoritary nucleotide was between 99.4-99.9% (with minimum values between 80.3-98.7%),
188 ruling out the concurrent presence of two variants in the samples either due to co-infection or
189 to contamination. In this SARS-CoV-2 recombinant, most of the spike gene was replaced in a
190 Delta 21J/AY.4 matrix by an Omicron 21K/BA.1 sequence (**Figures 1a, b, c**). Indeed, the
191 recombination sites were located between nucleotide positions 22,034 and 22,194 for the first
192 one, and between nucleotide positions 25,469 and 25,584 for the second one. These regions
193 corresponds to amino acids 158 to 211 of the spike protein and to amino acids 26 to 64 of the
194 ORF3a protein whose gene is contiguous to the spike gene. The Simplot recombination
195 analysis tool provided congruent results.

196 Genomes from two of the three patients were identical and clustered in the
197 phylogenetic analysis (**Figures 1d, e**) despite no epidemiological link was documented
198 between these two patients. The third genome exhibited 5 nucleotide differences.
199 Phylogenetic analyses showed that most of the recombinant genomes was most closely related
200 to Delta 21J/AY.4 variant genomes identified in our institute, while the region spanning a
201 large part of their spike gene was most closely related to Omicron 21K/BA.1 variant genomes
202 identified in our institute.

203 The respiratory sample from which the first recombinant genome was obtained was
204 inoculated on Vero E6 cells the day following recombinant identification, and cytopathic

205 effect was observed after 4 days (**Figures 2a, b**; collection of strains of IHU Méditerranée
206 Infection, no. IHUMI-6070VR). The same day, supernatant was collected and next-generation
207 genome sequencing was performed using Nanopore technology on a GridION instrument
208 after PCR amplification with Artic primers, which allowed obtaining the genome sequence of
209 the viral isolate 8 h later [GenBank Accession no. OM991295
210 (<https://www.ncbi.nlm.nih.gov/genbank/>)³⁰; available on the IHU Méditerranée Infection
211 website (<https://www.mediterranee-infection.com/sars-cov-2-recombinant/>)]. At mutated
212 positions compared to the Wuhan-Hu-1 isolate genome, mean sequencing depth was 2,771
213 reads and mean prevalence of the majoritary nucleotide was 99.1% (minimum, 95.1%), and
214 the consensus genome was identical to that obtained from the respiratory sample, showing
215 unambiguously that the virus isolated was the Delta 21J/AY.4-Omicron 21K/BA.1
216 recombinant. Finally, viral particles were observed in the culture supernatant by scanning
217 electron microscopy with a SU5000 microscope within minutes after supernatant collection
218 (**Figure 2c**).

219 The overall structure of the recombinant spike protein was predicted (**Figures 3a-c**).
220 When superimposed with the spike of the Omicron 21K/BA.1 variant, the main structural
221 changes were located in the N-terminal domain (NTD). In this region, the surface of the
222 recombinant spike protein is enlarged, flattened, and more electropositive, a property that is
223 characteristic of the Delta 21J/AY.4 NTD (**Figure 3c**). In the initial interaction of the virus
224 with the plasma membrane of the host cells, the NTD is attracted by lipid rafts, which
225 provides an electronegative landing platforms for the spike.^{38,39} Thus, an increase in the
226 electrostatic surface of the NTD is expected to accelerate the binding of the virus to lipid rafts,
227 which may confer a selective kinetic advantage against virus competitors.³⁸ The receptor
228 binding domain (RBD) of the recombinant is clearly inherited from the Omicron 21K/BA.1
229 variant (**Figure 3c**). The consequence is also an increase in the electrostatic surface potential

230 of the RBD, which may facilitate the interaction with the electronegative interface of the
231 ACE-2 cellular receptor. Overall, this structural analysis suggests that the recombinant virus
232 could have been selected on the basis of kinetic properties conferred by a convergent increase
233 of the electrostatic potential of both the NTD and the RBD, together with an enlargement of
234 the NTD surface, all features that suggest an optimization of virus binding to the host cell
235 membrane.

236 Currently used qPCR screening assays were not able to discriminate this Delta
237 21J/AY.4-Omicron 21K/BA.1 recombinant and the Omicron 21K/BA.1 variant because the
238 Delta variant signature mutation detected is absent from the recombinant genome. Therefore,
239 we attempted to promptly implement a specific qPCR assay that could be used to detect the
240 recombinant for routine diagnosis use. This was achieved in one day by selecting qPCR
241 systems from our toolbox of dozens of in house qPCR systems that were designed since the
242 emergence of the first variant during summer 2020 to specifically target SARS-CoV-2
243 variants or mutants.^{3,40} Two systems that target either the Delta 21J variant or the Omicron
244 BA.1 variant were combined in a duplex qPCR that can screen for the recombinant. In
245 preliminary assessment, both tested recombinant-positive samples were positive for the Delta
246 21J and Omicron BA.1 targets. In addition, 7 Delta non-21J-positive samples were negative
247 for both targets, 4 Delta 21J-positive samples were positive for the Delta 21J target but
248 negative for the Omicron BA.1 target, and 3 Omicron BA.1-positive samples were negative
249 for the Delta 21J target but positive for the Omicron BA.1 target.

250

251 **Discussion**

252 It is increasingly demonstrated that the genomes of most biological entities, whatever
253 their level of complexity, are mosaics of sequences from various origins.⁴¹⁻⁴⁵ The present
254 observations show us in real life the recombination potential of SARS-CoV-2, already largely

255 established for other coronaviruses.^{4-6,8,46} and reported or suspected for SARS-CoV-2.^{10,12,14-24}
256 SARS-CoV-2 recombinations were difficult to spot when only genetically very similar
257 viruses were circulating, as was the case in Europe during the first epidemic episode with
258 mutants derived from the Wuhan-Hu-1 virus. The increasing genetic diversity of SARS-CoV-
259 2, the tremendous number of infections at global and national levels, and the unprecedented
260 global effort of genomic sequencing (<https://covariants.org/per-country>),^{3,25,47} raised the
261 probability of detecting recombinants. Such observations will probably make it possible in the
262 short or medium term to assess the recombination rate of SARS-CoV-2, whether there are
263 recombination hotspots, and to what extent recombinations between different variants can
264 generate new viable, and epidemic variants. This questions on the impact of recombinations
265 on viral replication and transmissibility, and on clinical severity, as well as on the virus ability
266 to escape neutralizing antibodies elicited by vaccines or a previous infection. In this view,
267 culture isolation of SARS-CoV-2 recombinants as was carried out here for the first time to
268 our knowledge is of primary importance. This variant mentioned recently has no known
269 epidemic potential. This will allow studying their phenotypic properties, among which their
270 replicative capacity in various cell lines, their sensitivity to antibodies, or their genetic
271 evolution *in vitro*. Concurrently, a high level of genomic surveillance must be maintained in
272 order to detect and characterize all recombination events and circulating recombinants, which
273 is a critical scientific and public health issue.

274

275

276 **Acknowledgments**

277 We are very grateful to Clio Grimaldier, Rita Zgheib, Claudia Andrieu, Ludivine Bréchar,
278 Raphael Tola, Anthony Fontanini, and Jacques Bou Khalil for their technical help.

279 **Author contributions**

280 Study conception and design: Philippe Colson, Pierre-Edouard Fournier, Jacques Fantini,
281 Didier Raoult, Bernard La Scola. Materials, data and analysis tools: Philippe Colson, Pierre-
282 Edouard Fournier, Jeremy Delerce, Matthieu Million, Marielle Bedotto, Linda Houhamdi,
283 Nouara Yahy, Jeremy Bayette, Jacques Fantini. Data analyses: Philippe Colson, Pierre-
284 Edouard Fournier, Jeremy Delerce, Marielle Bedotto, Anthony Levasseur, Jacques Fantini,
285 Didier Raoult, Bernard La Scola. Writing of the first draft of the manuscript: Philippe Colson,
286 Jacques Fantini, and Pierre-Edouard Fournier. All authors read, commented on, and approved
287 the final manuscript.

288 **Funding**

289 This work was supported by the French Government under the “Investments for the Future”
290 program managed by the National Agency for Research (ANR), Méditerranée-Infection 10-
291 IAHU-03; by Région Provence Alpes Côte d’Azur and European funding FEDER PRIMMI
292 (Fonds Européen de Développement Régional-Plateformes de Recherche et d’Innovation
293 Mutualisées Méditerranée Infection), FEDER PA 0000320 PRIMMI; by Hitachi High-
294 Technologies Corporation, Tokyo, Japan; and by the French Ministry of Higher Education,
295 Research and Innovation (ministère de l’Enseignement supérieur, de la Recherche et de
296 l’Innovation) and the French Ministry of Solidarity and Health (Ministère des Solidarités et de
297 la Santé).

298 **Data availability**

299 The dataset generated during the current study is available from the GenBank database
300 (<https://www.ncbi.nlm.nih.gov/genbank/>)³⁰ (GenBank Accession no. OM990851, OM990852,
301 OM991095, OM991295) and from the IHU Méditerranée Infection website
302 (<https://www.mediterranee-infection.com/sars-cov-2-recombinant/>).

303 **Conflicts of interest**

304 Didier Raoult has a conflict of interest as having been a consultant for Hitachi High-

305 Technologies Corporation, Tokyo, Japan from 2018 to 2020. He is a scientific board member
306 of Eurofins company and a founder of a microbial culture company (Culture Top). All other
307 authors have no conflicts of interest to declare. Funding sources had no role in the design and
308 conduct of the study; collection, management, analysis, and interpretation of the data; and
309 preparation, review, or approval of the manuscript.

310 **Ethics**

311 This study has been approved by the ethics committee of the University Hospital Institute
312 Méditerranée Infection (No. 2022-001). Access to the patients' biological and registry data
313 issued from the hospital information system was approved by the data protection committee
314 of Assistance Publique-Hôpitaux de Marseille (APHM) and was recorded in the European
315 General Data Protection Regulation registry under number RGPD/APHM 2019-73.

316

317

REFERENCES

- 318 1. Lemey P, Ruktanonchai N, Hong SL, et al. Untangling introductions and persistence in
319 COVID-19 resurgence in Europe. *Nature*. 2021;595:713-717.
- 320 2. Hodcroft EB, Zuber M, Nadeau S, et al.. Emergence and spread of a SARS-CoV-2
321 variant through Europe in the summer of 2020. *Nature*. 2021;595:707-712.
- 322 3. Colson P, Fournier PE, Chaudet H, et al. Analysis of SARS-CoV-2 variants from
323 24,181 patients exemplifies the role of globalization and zoonosis in pandemics. *Front*
324 *Microbiol*. 2022b;12:786233.
- 325 4. Lai MMC. Recombination in large RNA viruses: Coronaviruses. *Semin Virol*.
326 1996;7:381-388.
- 327 5. Zhang Y, Li J, Xiao Y, et al. Genotype shift in human coronavirus OC43 and
328 emergence of a novel genotype by natural recombination. *J Infect*. 2015;70:641-50.
- 329 6. Xiao Y, Rouzine IM, Bianco S, et al. RNA recombination enhances adaptability and is
330 required for virus spread and virulence. *Cell Host Microbe*. 2017;22:420.
- 331 7. So RTY, Chu DKW, Miguel E, et al. Diversity of dromedary camel coronavirus
332 HKU23 in African camels revealed multiple recombination events among closely
333 related betacoronaviruses of the subgenus Embecovirus. *J Virol*. 2019;93:e01236-19.
- 334 8. Gribble J, Stevens LJ, Agostini ML, et al. The coronavirus proofreading
335 exoribonuclease mediates extensive viral recombination. *PLoS Pathog*.
336 2021;17(1):e1009226.
- 337 9. Bentley K, Evans DJ. Mechanisms and consequences of positive-strand RNA virus
338 recombination. *J Gen Virol*. 2018;99:1345-1356.
- 339 10. Jackson B, Boni MF, Bull MJ, et al. Generation and transmission of interlineage
340 recombinants in the SARS-CoV-2 pandemic. *Cell*. 2021;184:5179-5188.e8.

- 341 11. Francisco RDS Jr, Benites LF, Lamarca AP, et al. Pervasive transmission of E484K and
342 emergence of VUI-NP13L with evidence of SARS-CoV-2 co-infection events by two
343 different lineages in Rio Grande do Sul, Brazil. *Virus Res.* 2021;296:198345.
- 344 12. Taghizadeh P, Salehi S, Heshmati A, et al. Study on SARS-CoV-2 strains in Iran
345 reveals potential contribution of co-infection with and recombination between different
346 strains to the emergence of new strains. *Virology.* 2021;562:63-73.
- 347 13. Rockett, JD, Mailie G, Eby MS, et al. Co-infection with SARS-CoV-2 Omicron and
348 Delta Variants revealed by genomic surveillance. *medRxiv* 2022; 2022.02.13.22270755;
349 doi: <https://doi.org/10.1101/2022.02.13.22270755>.
- 350 14. Yi H. 2019 Novel coronavirus is undergoing active recombination. *Clin Infect Dis.*
351 2020;71:884-887.
- 352 15. Yeh TY, Contreras GP. Emerging viral mutants in Australia suggest RNA
353 recombination event in the SARS-CoV-2 genome. *Med J Aust.* 2020;213:44-44.e1.
- 354 16. VanInsberghe D, Neish AS, Lowen AC, Koelle K. Recombinant SARS-CoV-2
355 genomes are currently circulating at low levels. *bioRxiv* 2021;2020.08.05.238386. doi:
356 10.1101/2020.08.05.238386.
- 357 17. Gallaher WR. A palindromic RNA sequence as a common breakpoint contributor to
358 copy-choice recombination in SARS-COV-2. *Arch Virol.* 2020;165:2341-2348.
- 359 18. Haddad D, John SE, Mohammad A, et al. SARS-CoV-2: Possible recombination and
360 emergence of potentially more virulent strains. *PLoS One.* 2021;16:e0251368.
- 361 19. Makarenkov V, Mazoure B, Rabusseau G, Legendre P. Horizontal gene transfer and
362 recombination analysis of SARS-CoV-2 genes helps discover its close relatives and
363 shed light on its origin. *BMC Ecol Evol.* 2021;21:5.
- 364 20. Varabyou A, Pockrandt C, Salzberg SL, Pertea M. Rapid detection of inter-clade
365 recombination in SARS-CoV-2 with Bolotie. *Genetics.* 2021;218:iyab074.

- 366 21. Leary S, Gaudieri S, Parker MD, et al. Generation of a novel SARS-CoV-2 sub-
367 genomic RNA due to the R203K/G204R variant in nucleocapsid: homologous
368 recombination has potential to change SARS-CoV-2 at both protein and RNA level.
369 *Pathog Immun.* 2021;6:27-49.
- 370 22. Lohrasbi-Nejad A. Detection of homologous recombination events in SARS-CoV-2.
371 *Biotechnol Lett.* 2022 Jan 17:1–16. doi: 10.1007/s10529-021-03218-7. Epub ahead of
372 print.
- 373 23. Kreier F. Deltacron: the story of the variant that wasn't. *Nature.* 2022;602:19.
- 374 24. Ignatieva A, Hein J, Jenkins PA. Ongoing recombination in SARS-CoV-2 revealed
375 through genealogical reconstruction. *Mol Biol Evol.* 2022;39:msac028.
- 376 25. Aksamentov I, Roemer C, Hodcroft EB, Neher RA. Nextclade: clade assignment,
377 mutation calling and quality control for viral genomes. *Zenodo* 2021. doi:
378 <https://doi.org/10.5281/zenodo.5607694>.
- 379 26. Hadfield J, Megill C, Bell SM, et al. Nextstrain: real-time tracking of pathogen
380 evolution. *Bioinformatics.* 2018;34:4121-4123.
- 381 27. Rambaut A, Holmes EC, O'Toole Á, et al. A dynamic nomenclature proposal for SARS-
382 CoV-2 lineages to assist genomic epidemiology. *Nat Microbiol.* 2020;5:1403-1407.
- 383 28. Colson P, Delerce J, Beye M, et al. First cases of infection with the 21L/BA.2 Omicron
384 variant in Marseille, France. *medRxiv* 2022a; 2022.02.08.22270495; doi:
385 <https://doi.org/10.1101/2022.02.08.22270495>.
- 386 29. Houhamdi L, Gautret P, Hoang VT, Fournier PE, Colson P, Raoult D. Characteristics of
387 the first 1119 SARS-CoV-2 Omicron variant cases, in Marseille, France, November-
388 December 2021. *J Med Virol.* 2022 Jan 20. doi: 10.1002/jmv.27613. Epub ahead of
389 print.

- 390 30. Sayers EW, Cavanaugh M, Clark K, Pruitt KD, Schoch CL, Sherry ST, Karsch-
391 Mizrachi I. GenBank. *Nucleic Acids Res.* 2022 Jan 7;50(D1):D161-D164.
- 392 31. Lole KS, Bollinger RC, Paranjape RS, Gadkari D, Kulkarni SS, Novak NG, Ingersoll R,
393 Sheppard HW, Ray SC. Full-length human immunodeficiency virus type 1 genomes
394 from subtype C-infected seroconverters in India, with evidence of intersubtype
395 recombination. *J Virol.* 1999 Jan;73(1):152-60.
- 396 32. Nguyen LT, Schmidt HA, von Haeseler A, Minh BQ. IQ-TREE: a fast and effective
397 stochastic algorithm for estimating maximum-likelihood phylogenies. *Mol Biol Evol.*
398 2015 Jan;32(1):268-74. doi: 10.1093/molbev/msu300. Epub 2014 Nov 3. PMID:
399 25371430; PMCID: PMC4271533.
- 400 33. Kumar S, Stecher G, Li M, Knyaz C, Tamura K. MEGA X: Molecular Evolutionary
401 Genetics Analysis across Computing Platforms. *Mol Biol Evol.* 2018 Jun 1;35(6):1547-
402 1549. doi: 10.1093/molbev/msy096. PMID: 29722887; PMCID: PMC5967553.
- 403 34. Katoh K, Misawa K, Kuma K, Miyata T. MAFFT: a novel method for rapid multiple
404 sequence alignment based on fast Fourier transform. *Nucleic Acids Res.* 2002 Jul
405 15;30(14):3059-66. doi: 10.1093/nar/gkf436. PMID: 12136088; PMCID: PMC135756.
- 406 35. Altschul SF, Gish W, Miller W, Myers EW, Lipman DJ. Basic local alignment search
407 tool. *J Mol Biol.* 1990;215:403-10.
- 408 36. La Scola B, Le Bideau M, Andreani J, et al. Viral RNA load as determined by cell
409 culture as a management tool for discharge of SARS-CoV-2 patients from infectious
410 disease wards. *Eur J Clin Microbiol Infect Dis.* 2020;39:1059-1061.
- 411 37. Colson P, Lagier JC, Baudoin JP, Bou Khalil J, La Scola B, Raoult D. Ultrarapid
412 diagnosis, microscope imaging, genome sequencing, and culture isolation of SARS-
413 CoV-2. *Eur J Clin Microbiol Infect Dis.* 2020 Aug;39(8):1601-1603.

- 414 38. Fantini J, Yahi N, Azzaz F, Chahinian H. Structural dynamics of SARS-CoV-2 variants:
415 A health monitoring strategy for anticipating Covid-19 outbreaks. *J Infect.*
416 2021;83:197-206.
- 417 39. Fantini J, Yahi N, Colson P, Chahinian H, La Scola B, Raoult D. The puzzling
418 mutational landscape of the SARS-2-variant Omicron. *J Med Virol.* 2022 Jan 8. doi:
419 10.1002/jmv.27577. Epub ahead of print.
- 420 40. Bedotto M, Fournier PE, Houhamdi L, Colson P, Raoult D. Implementation of an in-
421 house real-time reverse transcription-PCR assay to detect the emerging SARS-CoV-2
422 N501Y variants. *J Clin Virol.* 2021;140:104868.
- 423 41. Raoult D. A viral grandfather: genomics in 2010 contradict Darwin's vision of
424 evolution. *Eur J Clin Microbiol Infect Dis.* 2011;30:935-6.
- 425 42. Merhej V, Raoult D. Rhizome of life, catastrophes, sequence exchanges, gene creations,
426 and giant viruses: how microbial genomics challenges Darwin. *Front Cell Infect*
427 *Microbiol.* 2012;2:113.
- 428 43. Feschotte C, Gilbert C. Endogenous viruses: insights into viral evolution and impact on
429 host biology. *Nat Rev Genet.* 2012;13:283-96.
- 430 44. Roux S, Enault F, Bronner G, Vaultot D, Forterre P, Krupovic M. Chimeric viruses blur
431 the borders between the major groups of eukaryotic single-stranded DNA viruses. *Nat*
432 *Commun.* 2013;4:2700.
- 433 45. Jacobs GS, Hudjashov G, Saag L, et al. Multiple deeply divergent Denisovan ancestries
434 in Papuans. *Cell.* 2019;177:1010-1021.e32.
- 435 46. Liu X, Shao Y, Ma H, et al. Comparative analysis of four Massachusetts type infectious
436 bronchitis coronavirus genomes reveals a novel Massachusetts type strain and evidence
437 of natural recombination in the genome. *Infect Genet Evol.* 2013;14:29-38.

438 47. Hodcroft E. 2012. CoVariants: SARS-CoV-2 mutations and variants of interest.

439 Available from: <https://covariants.org/>.

440

441
442
443
444
445
446
447
448
449
450
451
452
453
454
455
456
457
458
459
460
461
462
463
464
465

FIGURE LEGEND

Figure 1. Schematic of the SARS-CoV-2 Delta 21J/AY.4-Omicron 21K/BA.1 recombinant genome, and phylogenetic trees based on different regions of the Deltamicron genome reflecting the origin of most of the viral genome from a Delta 21J/AY.4 variant and the origin of a region spanning a large part of the spike gene from a Omicron 21K/BA.1 variant.

a: Map of the SARS-CoV-2 genome.

b: Schematic representation of parental and recombinant genomes.

c: Mutations in the three Delta 21J/AY.4-Omicron 21K/BA1 recombinant genomes. Adapted from screenshots of the nextclade web application output (<https://clades.nextstrain.org>).^{25,26}

Color codes for nucleotide mutations and are marked regions as follows: Green: U; yellow: G; blue: C; red: A; grey: deletions or uncovered regions. Genomes are labelled with the identifiers of the IHU Méditerranée Infection and the GenBank (<https://www.ncbi.nlm.nih.gov/genbank/>)³⁰ sequence databases.

d, e: Phylogenetic trees based on different regions of the Deltamicron genomes showing the origin of most of the viral genome from a Delta 21J/AY.4 variant (d) and the origin of a region spanning a large part of the spike gene from a Omicron 21K/BA.1 variant (e). The 10 genomes the most similar genetically to these regions of the recombinant genomes obtained here were selected from the sequence database of our institute through a BLAST³⁵ search, then were incorporated in the phylogeny together with the genome of the Wuhan-Hu-1 isolate. Sequences are labelled with the identifiers of the IHU Méditerranée Infection and the GenBank (<https://www.ncbi.nlm.nih.gov/genbank/>)³⁰ sequence databases.

Figure 2. Microscopy images of the virus cytopathic effect (a, b) and of a viral particle

466 **(c) in culture of the SARS-CoV-2 Delta 21J/AY.4-Omicron 21K/BA.1 recombinant on**
467 **Vero E6 cells.**

468 a. Absence of cytopathic effect (negative control: absence of virus); b. Cytopathic effect
469 observed 4 days post-inoculation on Vero E6 cells of the respiratory sample of the first patient
470 for whom the SARS-CoV-2 Delta 21J/AY.4-Omicron 21K/BA.1 recombinant was identified.
471 c. Scanning electron microscopy image was obtained with a SU5000 microscope (Hitachi
472 High-Technologies Corporation, Tokyo, Japan).

473

474 **Figure 3. Schematic of the predicted structure of the spike protein of the SARS-CoV-2**
475 **Delta 21J/AY.4-Omicron 21K/BA.1 recombinant**

476 a. Overall structure of the recombinant spike protein. The secondary structure is in grey,
477 mutated amino acids are in blue. NTD, N-terminal domain; RBD, receptor binding domain;
478 S1-S2, cleavage site.

479 b. Superimposition of the secondary structure of the Omicron 21K/BA.1 variant (in cyan) and
480 recombinant (in red) spike proteins. NTD, N-terminal domain; RBD, receptor binding
481 domain.

482 c. Comparison of the electrostatic surface potential of the spike proteins in Delta 21J/AY.4
483 lineage, Omicron 21K/BA.1 variant, and in the recombinant. The color scale (negative in red,
484 positive in blue, neutral in white) is indicated. NTD, N-terminal domain; RBD, receptor
485 binding domain.

486

487

488

TABLE

489
490
491

Table 1. Nucleotide and amino acid changes in the Deltamicron recombinant according to their presence/absence in the Delta 21J/AY.4 lineage and the Omicron 21K/BA.1 variant.

SARS-CoV-2 genes or genome regions	Nucleotide changes	Amino acid changes	Present in the Delta 21J/AY.4 lineage	Present in the Omicron 21K/BA.1 variant	Present in the Delta 21J/AY.4-Omicron 21K/BA.1 recombinant
5UTR	G210U	/	X		X
5UTR	C241U	/	X	X	X
ORF1a	A1321C	E352D			X
ORF1a	C3037U	/	X	X	X
ORF1a	G4181U	A1306S	X		X
ORF1a	C6402U	P2046L	X		X
ORF1a	C7124U	P2287S	X		X
ORF1a	C7851U	A2529V	X		X
ORF1a	A8723G	I2820V			X
ORF1a	C8986U	/	X		X
ORF1a	G9053U	V2930L	X		X
ORF1a	C10029U	T3255I	X	X	X
ORF1a	A11201G	T3646A	X		X
ORF1a	A11332G	/	X		X
ORF1b	C14407U	P314F / P314L			X
ORF1b	C14408U	P314F / P314L	X	X	X
ORF1b	U15264C	/	X		X
ORF1b	G15451A	G662S	X		X
ORF1b	C16466U	P1000L	X		X
ORF1b	C19220U	A1918V	X		X
S	C21618G	T19R	X		X
S	G21641U	A27S			X
S	C21846U	T95I	X	X	X
S	G21987A	G142D	X		X
S	GAGUUCA22028G	EFR156G	X		X
S	AAUU22193A	NL211I		X	X
S	U22204UGAGCCAGAA	Ins214EPE		X	X
S	G22578A	G339D		X	X
S	UC22673CU	S371L		X	X
S	U22679C	S373P		X	X
S	C22686U	S375F		X	X
S	G22813U	K417N		X	X
S	U22882G	N440K		X	X
S	G22898A	G446S		X	X
S	G22992A	S477N		X	X
S	C22995A	T478K	X	X	X
S	A23013C	E484A		X	X
S	A23040G	Q493R		X	X
S	G23048A	G496S		X	X
S	A23055G	Q498R		X	X
S	A23063U	N501Y		X	X
S	U23075C	Y505H		X	X
S	C23202A	T547K		X	X
S	A23403G	D614G	X	X	X
S	C23525U	H655Y		X	X
S	U23599G	N679K		X	X
S	C23604A	P681H		X	X
S	C23854A	N764K		X	X
S	G23948U	D796Y		X	X
S	C24130A	N856K		X	X
S	A24424U	Q954H		X	X
S	U24469A	N969K		X	X
S	C24503U	L981F		X	X
S	C25000U	/		X	X
ORF3a	C25667U	S92L			X
ORF3a	G25855U	D155Y			X
M	U26767C	I82T	X		X
ORF7a	U27638C	V82A	X		X
ORF7a	C27752U	T120I	X		X
ORF7b	C27874U	T40I	X		X
ORF8	AGAUUUC28247A	DF119Del	X		X
Intergenic region	UA28270U	/	X		X
N	A28461G	D63G	X		X
N	G28881U	R203M	X		X
N	G28916U	G215C	X		X
N	G29402U	D377Y	X		X
Intergenic region	G29540A	/			X
ORF10	G29645U	/			X
3UTR	G29742U	/	X		X

492
493

/, no change; Ins, insertion; Del, deletion; UTR, untranslated region; X, present. S gene region is indicated by a grey background.

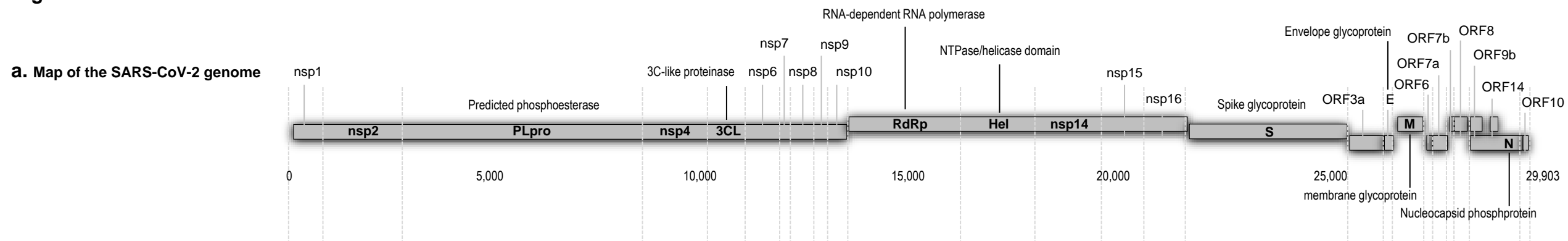
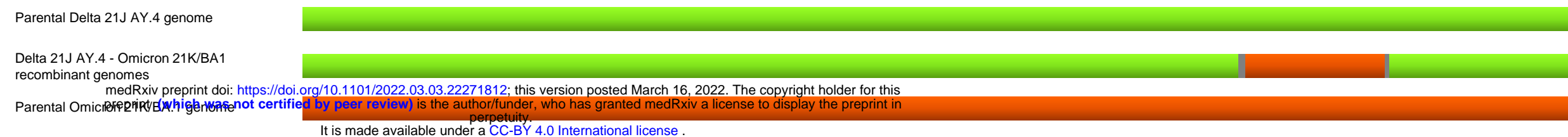
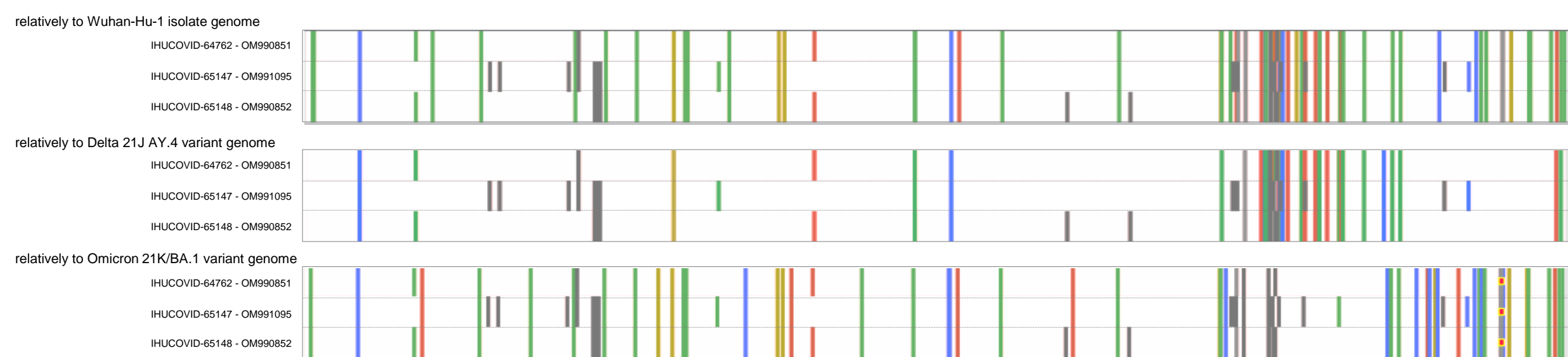
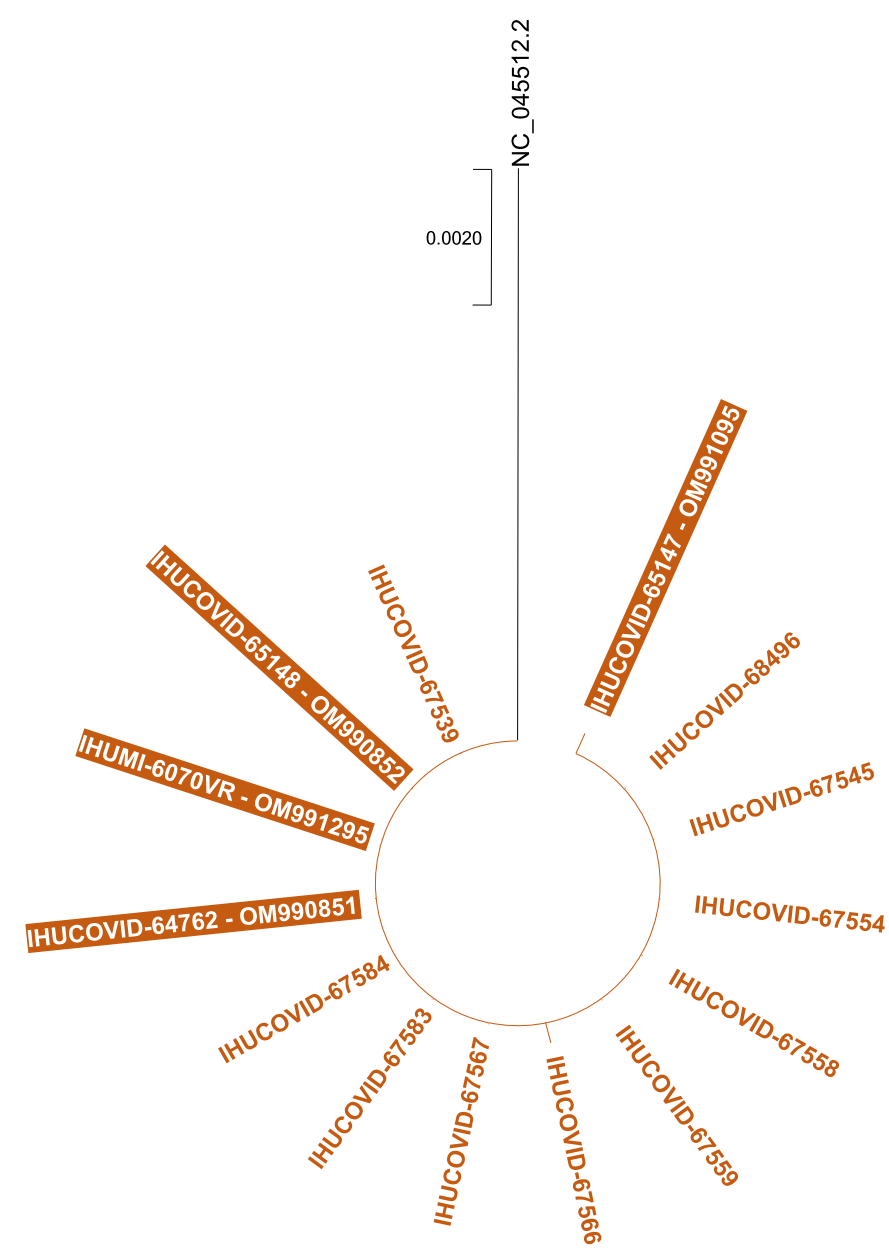
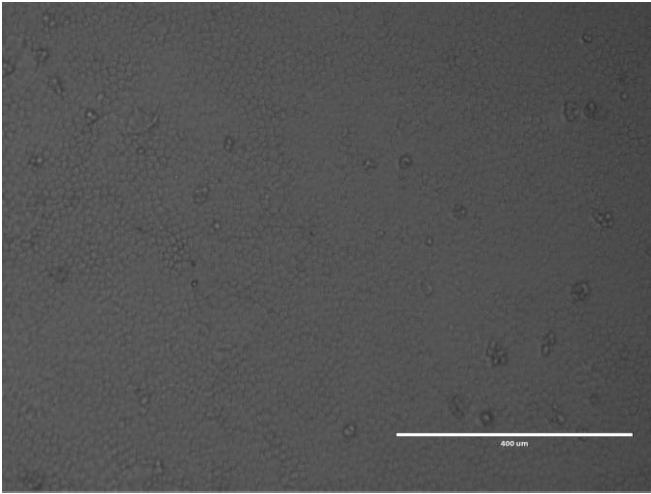
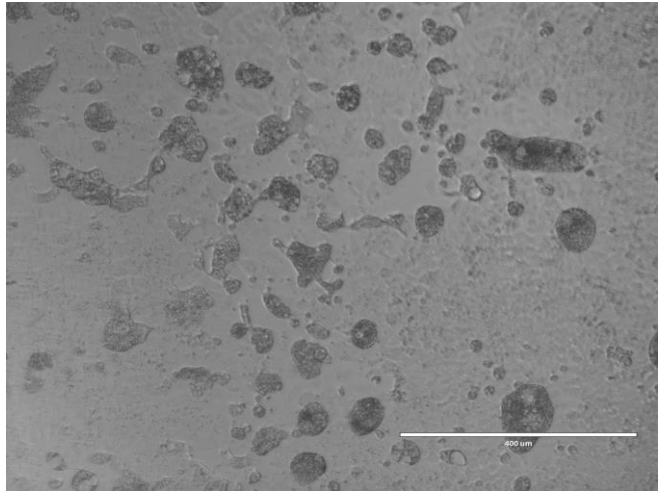
Fig. 1**b. Schematic of parental and recombinant genomes****c. Nucleotide mutations in the three Delta 21J AY.4 / Omicron 21K/BA1 recombinant genomes****d. Phylogeny based on the recombinant genomes excluding their Omicron 21K/BA.1 region****e. Phylogeny based on the Omicron 21K/BA.1 region of the recombinant genomes**

Fig. 2

a.



b.



c.

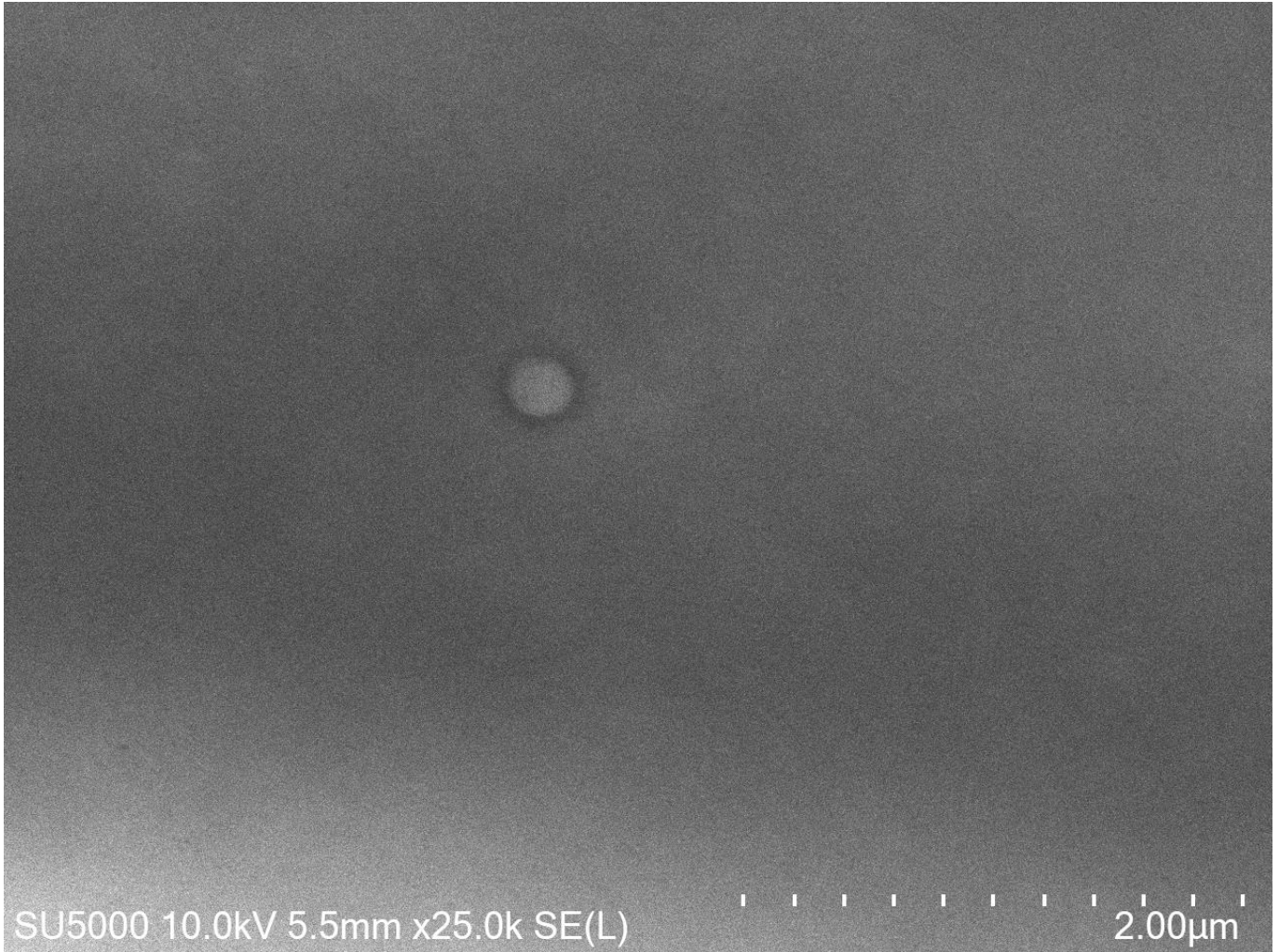


Fig. 3

